Defect Detection of Printing Images on Cans Based on SSIM and Chromatism

Maomin Zhou, Guijin Wang
Department of Electronic Engineering
Tsinghua University
Beijing, China
e-mail: zhoumaomin1576@163.com

Jinnan Wang, Changqing Hui, Wenming Yang
Department of Electronic Engineering, Graduate School
Tsinghua University
Shenzhen, China
e-mail: wangguijin@tsinghua.edu.cn

***Abstract*—In the production of digital printing equipment, it is a challenge to detect the printed surface defects of cylindrical surface like cans. This paper presents an automatic inspection program based on computer vision. We build a set of printing detection hardware system including the automatic image acquisition, high precision image registration. Then we propose a geometric defect detection based on SSIM and color defect detection algorithm based on CIEDE2000 color difference formula. The experimental results show that the system proposed by us has good effectiveness and robustness, and can realize digital detection and feedback adjustment.**

Keywords-image defect detection; registration; SSIM; color difference

I. INTRODUCTION

With the increase of modern technology, in the printing industry, more and more high-speed automated production methods are being used. People's requirements on the packaging printing pattern quality, especially cans surface image printing are higher. In the digital printing equipment production process, the evaluation and inspection of printing quality is a very important part. Accurate detection of image defects, such as scratches, stains, blur, color differences and other quality problems. Then the results are fed back to the printing module to realize the adjustment and optimization of printing process. These can reduce economic loss brought by mass production remarkably due to defect detection. Moreover, quality testing of color printing image is extraordinarily valuable to ensure good performance over manufactured products.

Many of the traditional defect detection are based on flat print detection, and the corresponding quality testing technology is relatively mature and perfect. J. L. Bouchot proposes an algorithm for automatic fault detection in textures, by comparing the defect image and the standard image based on the image matching method [1]. Some methods, based on the classification method, are to carry out defect detection through the feature extraction and classification including some machine learning methods [2-3]. Some are based on statistics. By calculating the mean, variance, histogram of the image, or two-dimensional information, such as the Gray Level Co-occurrence Matrix [4]. Some methods, based on Discrete Fourier Transform(DFT), are to transform the image to frequency domain and process [5]. But this method may add some complexity. The above detection methods are generally used for the defect detection of the content, while color defects detection are often ineffective. Moreover, the traditional detection is mainly for the printed objects on the plane, while detection effect of the curved surface or cylindrical surface is not very well. When it comes to the cans of cylindrical material, the image printing process on the surface of cans uses the rotary inkjet, working with high speed and jitter, which make color information more complex. The image acquisition and image registration requirements are higher [6-8], and due to the unstable speed, the impact of ambient light on the robustness of the defect detection algorithm is also a challenge.

In this paper, we mainly solve the surface image printing quality detection problems. Cans of this cylindrical bearing in the production of digital printing equipment are used as an example. We set up a simple cans printing detection hardware system, which utilizes the rotating motor to simulate the printing process of the cans. A prism split-beam high-speed linear array camera is used to overcome RGB three-channel color offset, and high brightness of the coaxial light source is applied to overcome the impact of environmental light interference. For the software algorithm, the standard images and the images to be detected are obtained for high-precision image registration, which can effectively overcome the impact of motor speed instability. For the defect detection, we divide the defects into geometric defects and color defects. Geometric defects evaluated by SSIM mainly include scratches, stains, blur and other line defects. Color defects are mainly the difference between the color of prints, and the chromatic aberration is assessed by the International Commission on illumination. We use the most common CIEDE2000 color formula to measure the color difference, which is detected via setting threshold. Experimental results show that our methods are featured with high accuracy and excellent robustness.

II. SYSTEM OVERVIEW

Our overall detection process is shown in Fig. 1. Firstly, the high-speed image data is acquired, qualified printing cans and the cans to be detected are scanned through the line scan camera. The second part is the data processing to register the images. The third step is defect detection, including the geometrical defects and color defects detection, which provides the detect results and feedback to the digital printing equipment.

978-1-5090-6351-2/17/$31.00 ©2017 IEEE

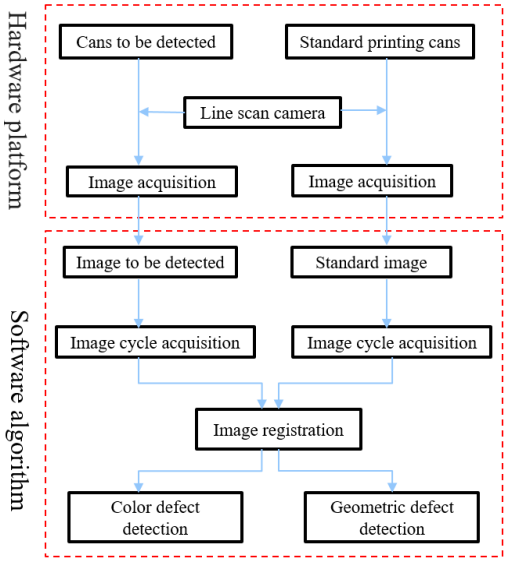

Figure 1. The structure of the system.

A. *Image Cycle Acquisition*

The image data scanned by the line array camera may contain a plurality of cycles and there is some redundant information in the original data stream due to the camera's view size. Therefore, it is necessary to process the original image data by removing the redundant boundary to get complete periodic images.

We use template matching method to obtain the images. At the beginning of the scanned images, a certain width of the local images is selected as template T(m*n). In the whole target image S(h*w) to search for images with similar information in the template, a cross-correlation detection is carried out when every time a move is made. After the whole image is traversed, the most similar point is regarded as the matching point. As long as its coordinate position is located, a complete period image is obtained.

When the width of both the image to be detected and the standard image is one cycle, as the period length of the template matching method is not accurate enough, so there will be some tiny differences in the length between the standard image and the image to be detected. Once the starting position of the two images is not the same, the need to shift the image for translating results in stitching gap between the initial image and the tail image during the registration process, which will lead to false inspection. Therefore, the solution we adopt is as follows: The standard image length is two cycles, while the image to be detected is one cycle, so the stitching gap can be avoided and the complexity of subsequent registration algorithm will not increase.

B. *Image Registration*

After the images are obtained, the registration of two images is needed. As the central axis of the can might not coincide with the rotating center of the motor and the speed of the motor is unstable, so there will be some fluctuations and the images in different places will have different distortions. Hence, it is not accurate to use the whole image for registration. We use the following methods to solve this problem.

Firstly, as the standard image is two cycles and the image to be detected is one cycle, we need to find the same starting position. We still use similar template matching method. We select a certain width of image to be detected in the starting area and locate the starting position where the similarity between the image to be detected and the standard image is the most.

The second is high-precision image registration. When the starting position of the two images is determined, we divide the image into multiple small width vertical blocks to overcome the above-mentioned problems due to the position offset and speed instability. Each block is individually registered, as the distortion is consistent across each block and that different block distortions may be different.

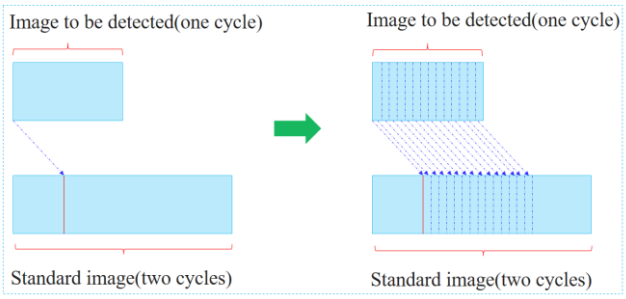

Figure 2. High-precision registration based on blocks.

As shown in Fig. 2, in the registration process of each block, there may be scale scaling between the two images. Besides the translation difference, we add a zoom factor between 0.8 and 1.2, whose step is 0.1, and a small range of translation for each block parameter. Combined with PSNR to calculate the two images corresponding block correlation coefficient, the PSNR of the blocks are traversed to find the maximum corresponding zoom parameters and translation parameters to achieve high-precision registration.

C. *Geometric Defect Detection*

In the process to detect geometric imperfections, some stains, blurring, scratches and so on, may occur in the production process. In order to detect as accurately and closely to human visual inspection, we adopt the image quality evaluation method based on structural similarity measure SSIM [9-10]. The method can objectively reflect the change of the structure information of the image.

The image evaluation method of SSIM mainly compares the standard image and the image to be detected from three aspects: brightness, contrast and structure similarity. Let x and y represent the standard image and the image to be detected respectively. The model is defined as:

$$\mathrm{SSIM} = [l(x,y)]^{\alpha}[c(x,y)]^{\beta}[s(x,y)]^{\lambda} \quad (1)$$

$$\mathrm{l(x,y)} = \frac{2\mu_x\mu_y + C_1}{\mu_x^2 + \mu_y^2 + C_1} \quad (2)$$

$$c(x,y) = \frac{2\sigma_x\sigma_y + C_2}{\sigma_x^2 + \sigma_y^2 + C_2} \tag{3}$$

$$s(x,y) = \frac{\sigma_{xy} + C_3}{\sigma_x\sigma_y + C_3} \tag{4}$$

where μ_x and μ_y are the mean values of x and y; σ_x and σ_y are the standard deviation of x and y; σ_{xy} is the covariance of x and y; C_1、C_2 *and* C_3 are very small positive numbers to prevent the situation that the denominator is zero due to instability.

For two images that have been registered, the SSIM of the two images is calculated by the formula above, and the larger the SSIM is, the more similar the corresponding information is. The smaller the SSIM is, the larger the difference is. By setting the empirical threshold and image binarization, we can detect various types of geometric defects.

D. Color Defect Detection

In the time when digital printing equipment is working, uneven pigment ink or nozzle clogging may result in color differences such as color heterogeneity or color cast, so it is necessary to detect the printed matter from the color point of view. But SSIM for color defects detection is not well, we need to find other ways to detect the color defects.

To quantify the color difference between the image to be detected and the standard image, the printing industries utilize the color printing method for quality inspection and control. The ideal chromatic aberration formula should be consistent with the visual experience of the human eye. CIEDE2000 color difference formula is the best color standard, as officially announced by the International Commission on Illumination (CIE) in 2000. It contains the brightness, hue and saturation of the integrated color perception of the standard. Therefore, we use CIEDE2000 to quantify the color difference [11-12].

1) Color space conversion

Firstly, it is necessary to convert the acquired RGB image to the CIE XYZ color space [13]. The linear transformation process is as follows:

$$\begin{bmatrix} X \\ Y \\ Z \end{bmatrix} = \begin{bmatrix} 0.412453 & 0.357580 & 0.180423 \\ 0.212671 & 0.715160 & 0.072169 \\ 0.019334 & 0.119193 & 0.950227 \end{bmatrix} \cdot \begin{bmatrix} R \\ G \\ B \end{bmatrix} \tag{5}$$

where R, G and B data are rescaled between 0 and 1.

Secondly, through the CIE XYZ color space to the CIE Lab color space, which is a non-linear transformation, the process is as follows:

$$\begin{aligned} L^* &= 116f\left(\frac{Y}{Y_0}\right) - 16 \\ a^* &= 500\left[f\left(\frac{X}{X_0}\right) - f\left(\frac{Y}{Y_0}\right)\right] \\ b^* &= 200\left[200f\left(\frac{Y}{Y_0}\right) - f\left(\frac{Z}{Z_0}\right)\right] \end{aligned} \tag{6}$$

Where

$$f(I) = \begin{cases} (I)^{1/3} & I > (6/29)^3 \\ \left(\frac{841}{108}\right) I + \frac{4}{29} & I \le (6/29)^3 \end{cases} \tag{7}$$

In the formula , X, Y, Z usually refers to the tristimulus values of the object color, X_0、Y_0、Z_0 are the tristimulus values of the CIE standard illuminator, under the D_{65} standard light source, $X_0 = 95.045$、$Y_0 = 100$、$Z_0 = 108.892$.

2) Color difference calculation

Images are converted into the CIE Lab color space, then the standard map and reference picture of the color are calculated using CIEDE2000 color formula, as shown below:

$$\Delta E_{00} = \sqrt{\left(\frac{\Delta L'}{K_L S_L}\right)^2 + \left(\frac{\Delta C'_{ab}}{K_C S_C}\right)^2 + \left(\frac{\Delta H'_{ab}}{K_H S_H}\right)^2 + R_T\left(\frac{\Delta C'_{ab}}{K_C S_C}\right)\left(\frac{\Delta H'_{ab}}{K_H S_H}\right)} \tag{8}$$

Where $\Delta L', \Delta C'_{ab}, \Delta H'_{ab}$ are calculated by L^*, a^*, b^*, which, respectively, represent the brightness difference, saturation difference and hue difference. S_L, S_C, S_H are called as weighting functions. R_T represents the rotation angle which is determined by the hue. K_L, K_C, K_H are the correction parameters that are related to the use of conditions .In this paper, we take the standard value as $K_L = K_C = K_H = 1$.

Through the conversion of the color space and the calculation of the color difference, we can acquire the color difference between the image and the standard image to be detected, and then set a reasonable threshold to achieve the quantitative detection of color differences.

III. EXPERIMENTAL STUDY

A. Experimental Setup

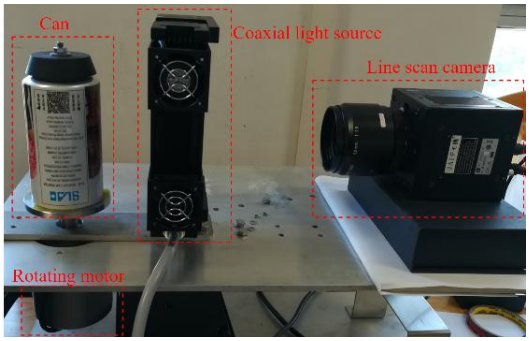

Figure 3. Hardware system platform.

In order to simulate the printing inspection in the production process of the real can, we set up a hardware platform, as shown in Fig. 3, which mainly includes a rotating motor, a can, a coaxial white light source, a JAI LT-200CL 3-CMOS color line scan camera, a Silicon software Me5 Marathon ACL Image acquisition card and a computer equipment. Our line scan camera is based on JAI's advanced prism technology, which is used to obtain high-quality scanning images to overcome the traditional RGB three-channel time-sharing imaging color shift and ensure that the

scanning process does not bring color effects. A coaxial white light source is used to provide more uniform and more uniform lighting and avoid the impact of the object caused by reflection and ambient light.

B. Simulation Results

In order to verify the validity and accuracy of the geometric defect algorithm and the color defect algorithm proposed by us, we first carry out the simulation experiment. We collect the scanned images from the hardware platform. Some simulations are directly added to the image through the software Defects, including different thickness of the lines, local blur, local color of the subtle changes. After that we develop the software algorithm for testing, and the experimental results are as follows:

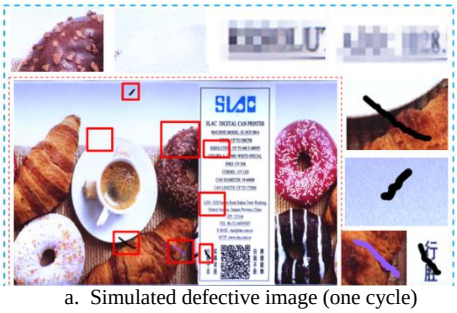

a. Simulated defective image (one cycle)

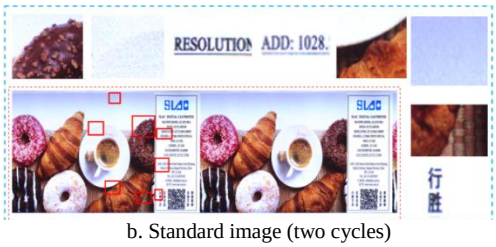

b. Standard image (two cycles)

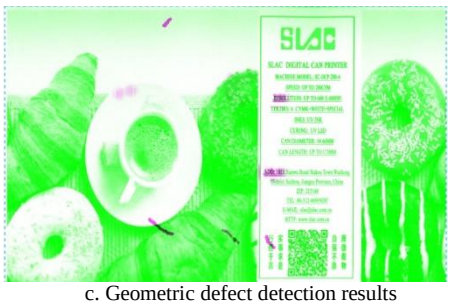

c. Geometric defect detection results

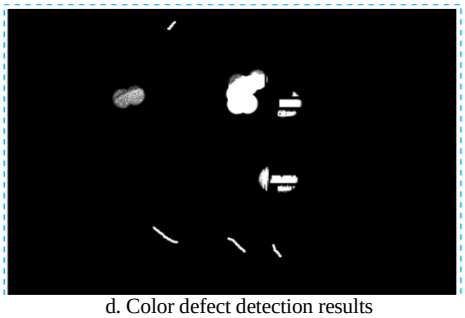

d. Color defect detection results

Figure 4. Results of simulation defects.

Fig. 4 shows the results of geometric defect detection based on SSIM, Fig. 4(a) represents of the simulation defects, Fig. 4(b) is the standard image, Fig. 4(c) represents the geometric defect detection results, while Fig. 4(d) shows the color defect detection results based on the CIEDE2000 color difference formula. All kinds of defects can be correctly detected, which proved the effectiveness and correctness of our algorithms.

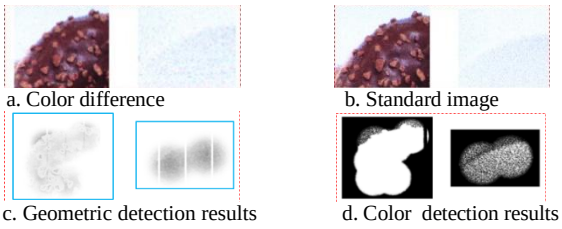

a. Color difference b. Standard image

c. Geometric detection results d. Color detection results

Figure 5. The necessity of color defect detection.

At the same time, comparing Fig. 5(c) and Fig. 5(d), we can also see that as for scratches, blur, stains and other geometric defects, we could acquire excellent results with SSIM. When it comes to color differences, the result of using SSIM is not obvious, however, the results of using CIEDE2000 color formula is better than SSIM, which proves that it is necessary to combine these two methods to detect the geometric defects and color defects.

After the simulation test, we carry out the real defect test, we select some practical defects cans, including some with scratches, stains, ink. The surface pattern of these cans are detected through the camera for comparison tests, the results are as follows.

C. Real Experimental Results

After the simulation test, we carry out the real defective test. The final and standard images for comparison test are as follows:

a. Real defective image (one cycle)

b. Standard image (two cycles)

Figure 6. Results of real defect detection.

As shown in Fig. 6, Fig. 6(a) shows the physical defects that exist on the real cans. Fig. 6(b) is the standard image. Defects include stains, scratches, and inks. The details of these defects are shown in the following figures. In order to prove our methods are effective, we make comparative

experiment by calculating absolute difference (AD) between the standard image and the image to be detected after registration.

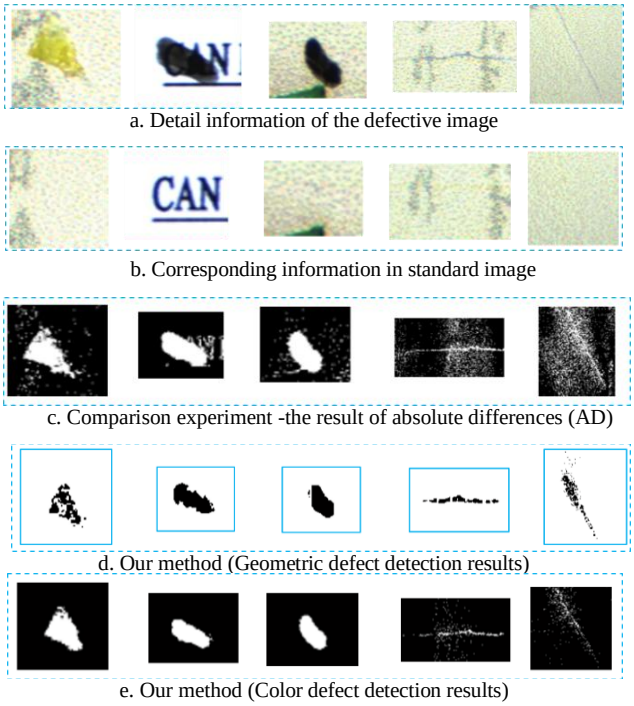

a. Detail information of the defective image

b. Corresponding information in standard image

c. Comparison experiment -the result of absolute differences (AD)

d. Our method (Geometric defect detection results)

e. Our method (Color defect detection results)

Figure 7. Experimental results and comparisons.

Fig. 7(a) shows the detail information of the defects in Fig. 6(a). Fig. 7(b) shows the corresponding information in Fig. 6(b). Fig.7(c) shows the result of absolute differences between the standard image and the image to be detected after registration. Fig. 7(d) shows the geometric defect detection results. Fig. 7(e) shows color defect detection results. We can see from the results that using absolute difference (AD) is not well in these detection, there are some other normal areas around the defects that have caused errors. Compared with AD, our methods can achieve better performance. The real defects can be correctly detected, which proved the effectiveness of our algorithms.

IV. CONCLUSION

This paper is mainly aimed at solving the problem of printing image defect detection in the industrial production of digital printing equipment. We propose a detection program based on computer vision and set up a set of hardware detection system platform through the use of line scan camera to capture images. And after high-precision image registration, we propose a geometric defect detection algorithm based on SSIM and a color defect detection algorithm based on CIEDE2000 color difference formula. We have carried out the simulation and the real test, results of which show that our algorithms can effectively achieve a variety of subtle defects detection, and overcome the motor speed instability, ambient light interference and other effects, with good robustness. In the future, we will feedback the test results to the printing equipment to achieve the iterative closed-loop optimization of the printing process adjustment.

ACKNOWLEDGMENT

This work was supported by Tsinghua University Initiative Scientific Research Program (2016SZ0306), in part by the National Natural Science Foundation of China under Grant 61671266, 61327902, in part by the Research Project of Tsinghua University under Grant 20161080084, and in part by National High-tech Research and Development Plan under Grant 2015AA042306.

REFERENCES

[1] J. L. Bouchot, G. Stübl and B. Moser, "A template matching approach based on the discrepancy norm for defect detection on regularly textured surfaces," In Quality Control by Artificial Vision Conference, QCAV. 2011.

[2] Kumar and H. C. Shen, "Texture inspection for defects using neural networks and support vector machines," Image Processing. 2002. Proceedings. 2002 International Conference on. Vol. 3. IEEE, 2002.

[3] L. Occhipinti, G. Spoto, M. Branciforte, and F. Doddo, "Defects detection and characterization by using cellular neural networks," in Proc.ISCAS, 2001, pp. 481–484.

[4] R. W. Conners , C. W. Mcmillin, K. Lin , and R. E. Vasquez-Espinosa, "Identifying and locating surface defects in wood: Part of an automated lumber processing system," IEEE Transactions on Pattern Analysis and Machine Intelligence, 1983(6), pp.573-583.

[5] D. M. Tsai, and C. Y. Hsieh, "Automated surface inspection for directional textures," Image and vision computing 18.1 ,1999, pp.49-62.

[6] B. He, G. Wang, X. Lin, C. Shi, and C. Liu, "High-accuracy sub-pixel registration for noisy images based on phase correlation, " IEICE TRANSACTIONS on Information and Systems 94.12 ,2011, pp.2541-2544.

[7] Q. Miao, G. Wang, and X. Lin, "Kernel based image registration incorporating with both feature and intensity matching," IEICE TRANSACTIONS on Information and Systems, 93(5), 2010,pp. 1317-1320.

[8] L. G. Brown, "A survey of image registration techniques," ACM computing surveys (CSUR) 24.4 ,1992, pp.325-376.

[9] Z. Wang, A. C. Bovik, H. R. Sheikh, and E. P. Simoncelli, "Image quality assessment: from error visibility to structural similarity," IEEE transactions on image processing 13.4 ,2004, pp. 600-612.

[10] A. Hore and D. Ziou, "Image quality metrics: PSNR vs. SSIM," Pattern recognition (icpr), 2010 20th international conference on. IEEE, 2010.

[11] G. Sharma, W. Wu, and E. N. Dalal, "The CIEDE2000 color‐difference formula: Implementation notes, supplementary test data, and mathematical observations," Color Research & Application 30.1 ,2005,pp. 21-30.

[12] Y. Yang, J. Ming, and N. Yu, "Color image quality assessment based on CIEDE2000," Advances in Multimedia 2012 ,2012, 11.

[13] R. V. Rossel, B. Minasny, P. Roudier, and A. B. McBratney, "Colour space models for soil science," Geoderma 133.3 ,2006, pp.320-337.